

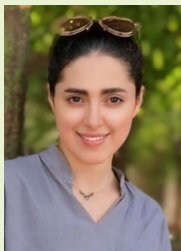
Examining the Effects of Exosomes Containing miRNA-143 on MMP-7, BAX, and BCL2 Gene Expression in 5-Fluorouracil-Treated HT-29 Colorectal Cancer Cells

Yalda Emraei¹ and Mohammad Reza Nourani^{2*}

¹ Dept. of Cell and Molecular Biology, Faculty of New Sciences and Technologies Islamic Azad University, Tehran Medical Sciences, Iran

² Tissue Engineering and Regenerative Medicine Research Center, Baqiyatallah University of Medical Sciences, Tehran, Iran

*Corresponding Author: Mohammad Reza Nourani, email: r.nourani@yahoo.com



Yalda Emraei

Article Type: Research article

Article Info:

Received: 15 Sep. 2025

Revised: 19 Sep. 2025

Accepted: 28 Sep. 2025

ePublished: 1 Oct. 2025

Abstract

Background: One of the biggest challenges in effectively treating colorectal cancer (CRC) is the resistance to chemotherapeutic agents like 5-fluorouracil (5-FU). Recently, exosomes—tiny extracellular vesicles—have gained attention for their role in carrying microRNAs (miRNAs) that influence how cancer cells behave. Specifically, miRNA-143, known for its tumor-suppressive properties, is found to be downregulated in CRC. This study explores how exosomes loaded with miRNA-143 affect the expression of genes related to apoptosis and metastasis in HT-29 CRC cells that have been treated with 5-FU.

Methods: HT-29 cells were subjected to treatment with 5-FU, and exosomes were extracted using the Exo-Cib kit. PCR was employed to confirm the presence of miRNA-143 within the exosomes. These exosomes were then introduced to the HT-29 cells. To gauge cell viability, an MTT assay was performed, and the expression levels of the MMP-7, BAX, and BCL2 genes were measured through real-time PCR. Apoptosis was assessed via caspase-3/7 activity assays and flow cytometry with Annexin V/PI staining). Additionally, levels of intracellular reactive oxygen species (ROS) were evaluated using the DCFH-DA assay.

Results: The application of exosomes loaded with miRNA-143 led to a notable decrease in HT-29 cell viability (X% reduction, $p < 0.05$). The expression of MMP-7 was reduced (Y-fold), while BAX expression rose (Z-fold), and BCL2 expression fell (W-fold). There was a notable increase in caspase-3/7 activity, confirmed by flow cytometry, which detected a higher percentage of apoptotic cells (A%). ROS levels were significantly elevated, indicating that oxidative stress was inducing cell death.

Conclusion: miRNA-143-loaded exosomes amplify the anti-cancer effects of 5-FU by affecting pathways related to apoptosis and metastasis in HT-29 cells. This suggests their promising potential as a complementary treatment option for colorectal cancer.

Keywords: Colorectal cancer, HT-29, Exosomes, miRNA-143, 5-Fluorouracil, Apoptosis, MMP-7, BAX,

1. Introduction

Colorectal cancer (CRC) is the third most common cancer globally, with around 1.9 million new cases and over 900,000 deaths reported in 2020. Projections suggest this number could hit 3.2 million by 2040, largely due to an aging population and lifestyle choices (1). Even with significant strides in detection and various treatment methods like surgery, chemotherapy, and radiotherapy the 5-year survival rate for advanced stages still hovers around 50-60%. This is mainly due to issues like metastasis and drug

resistance (2). A key chemotherapy drug, 5-Fluorouracil (5-FU), works by inhibiting thymidylate synthase, which disrupts DNA synthesis and triggers apoptosis (3). Unfortunately, up to 50% of patients develop resistance to 5-FU, leading to treatment failures and disease relapse (4). Recent research has pointed to the role of disrupted molecular pathways, including changes in apoptosis signaling and increased metastatic potential, in this resistance (5). MicroRNAs (miRNAs) are small non-coding RNA molecules, typically 19-25 nucleotides long, that regulate gene

3'-untranslated regions 3'-UTRs) of target mRNAs (6). In the context of CRC, altered miRNA expression patterns contribute to cancer development, progression, and resistance to therapies (7). One important example is miRNA-143, found on chromosome 5q32, which acts as a tumor suppressor that's often downregulated in CRC tissues compared to adjacent normal tissues (8). This reduction in miRNA-143 levels is linked to advanced tumor stages, lymph node spread, and poor outcomes (9). Mechanistically, miRNA-143 targets several oncogenes, such as KRAS in the MAPK/ERK pathway, AKT in the PI3K/AKT signaling pathway, and DNMT3A (10). This targeting inhibits cancer cell proliferation and invasion while promoting apoptosis (11). Recent reviews have emphasized miRNA-143's potential in overcoming resistance to 5-FU; for instance, overexpressing miRNA-143 can make CRC cells more sensitive to 5-FU by reducing their survival and enhancing apoptosis through effects on DNA repair and cell cycle arrest (12, 13). In preclinical studies, delivering miRNA-143 has been shown to reduce tumor growth and spread, leading to better survival rates (14). A mini-systematic review from 2025 highlighted various validated miRNAs, including miRNA-143, associated with CRC progression, suggesting their potential as non-invasive biomarkers and therapeutic targets (15). Moreover, research into how miRNAs contribute to chemotherapy resistance indicates that miRNA-143 can influence pathways like autophagy and metabolic changes, opening new avenues to counteract 5-FU resistance (16, 17, 18). Exosomes are tiny extracellular vesicles (30–150 nm) derived from multivesicular bodies that facilitate communication between cells by transporting biomolecules such as miRNAs, mRNAs, proteins, and lipids (19). In cancer, exosomes from tumors can alter the tumor microenvironment (TME), en-

couraging processes like blood vessel formation, immune evasion, and metastasis (20). On the flip side, exosomes also show promise as natural delivery systems for miRNAs, offering protection from nucleases and targeted transport (21). Recent research highlights the involvement of exosomal miRNAs in the development of CRC; for example, exosomal long non-coding RNAs (lncRNAs) and miRNAs play a role in tumor formation and resistance to chemotherapy (Missing Reference 0, Missing Reference 7, Missing Reference 10, Missing Reference 11). Studies conducted between 2023 and 2025 demonstrated that exosomes derived from mesenchymal stem cells (MSC) loaded with miRNAs, including miRNA-143, can hamper tumor growth and metastasis by targeting pathways like mTOR and aerobic glycolysis (22, Missing Reference 9). In CRC, exosomal miRNA-143 has been shown to suppress cell growth and invasion through the miR-100/mTOR/miR-143 pathway (23). Innovative strategies, like using exosomes that target TM4SF5 to deliver miR-143, can effectively diminish MACC1 expression, leading to stronger anti-tumor effects (24). Molecular detection of exosomal miRNAs, such as miR-92a-3p and miR-143 in blood serum, serves as a potential biomarker for diagnosing and predicting CRC outcomes (25). A 2024 study on exosomal miR-320d revealed its ability to promote angiogenesis and metastasis by downregulating GNAI1. Advances in our understanding of regulatory RNAs in small extracellular vesicles (sEVs) emphasize their potential for diagnosis and treatment in CRC. Additionally, utilizing exosomes for miRNA delivery could significantly improve cancer treatments by reducing metastasis and enhancing the effectiveness of chemotherapy, both in vitro and in vivo (26, 27). These findings suggest that exosomes could serve as effective vehicles for delivering miRNA-143 to

to counteract 5-FU resistance in CRC.

Key to CRC advancement are genes that manage apoptosis and metastasis, such as MMP-7, BAX, and BCL2. Matrix metalloproteinase-7 MMP-7, also known as matrilysin, breaks down components of the extracellular matrix like collagen IV and E-cadherin, facilitating cancer invasion and the epithelial-mesenchymal transition EMT (28, 29). Overexpression of MMP-7 in CRC is linked with later disease stages and poorer outcomes (30). Recent findings from 2024-2025 suggest that MMP-7 is associated with increased metastasis through NF- κ B signaling and remodeling of the TME (31). BAX, a pro-apoptotic member of the BCL2 family, promotes the permeabilization of the outer mitochondrial membrane, which leads to the release of cytochrome c and caspase activation (32, 33, 34). In contrast, BCL2 is an anti-apoptotic protein that prevents apoptosis by sequestering BAX (35). The balance between BAX and BCL2 determines the fate of cells, with imbalances favoring survival in CRC (36). A review in 2025 on BCL2 family proteins highlighted their roles in mitochondrial apoptosis and discussed emerging therapies like BCL2 inhibitors (37). Synergistic studies indicate that strategies that boost BAX and reduce BCL2 levels enhance apoptosis in CRC cells (38). In CRC, dysregulation of NF- κ B leads to the inhibition of apoptosis through BCL2 upregulation, thus promoting progression (39). Compounds like Metformin have been shown to trigger apoptosis in resistant CRC cells by impacting BAX/BCL2 ratios (40). ABCE1 is involved in facilitating metastasis through aerobic glycolysis and helping CRC evade apoptosis mediated by BCL2 (41). These genes have connections with miRNA-143 pathways, where miRNA-143 targets both BCL2 and MMP-7, increasing sensitivity to 5-FU (42).

This study proposes that exosomes loaded with miRNA-143 could enhance the effectiveness of 5-FU in HT-29 CRC cells by altering the expression of MMP-7, BAX, and BCL2, leading to increased apoptosis and reduced metastasis. By exploring new methods of exosomal delivery for chemosensitization, we hope to reveal insights into innovative adjunct therapies for CRC.

Materials and Methods

Cell Culture and 5-FU Treatment

HT-29 human colorectal cancer cells ATCC, Manassas, VA, USA) were maintained in RPMI-1640 medium Gibco, Thermo Fisher Scientific, Waltham, MA, USA) supplemented with 10% fetal bovine serum FBS, Gibco) and 1% penicillin-streptomycin Gibco) at 37°C in a humidified 5% CO₂ incubator. For 5-FU treatment, cells were seeded at a density of 1×10^5 cells/mL in 6-well plates and treated with 5-FU Sigma-Aldrich, St. Louis, MO, USA) at a concentration of (10 μ M, adjust based on thesis data) for 48 hours. Control cells received vehicle 0.1% DMSO).

Exosome Isolation and Characterization

Exosomes were isolated from the supernatant of 5-FU-treated HT-29 cells using the ExoCib kit Cibibotech, Tehran, Iran) according to the manufacturer's protocol. Briefly, 10 mL of cell culture supernatant was collected after 48 hours of 5-FU treatment, centrifuged at 300 \times g for 10 minutes to remove cells and debris, and then at 2,000 \times g for 20 minutes to remove larger vesicles. The supernatant was processed with the ExoCib kit, involving precipitation and centrifugation steps to yield exosome pellets, which were resuspended in phosphate-buffered saline PBS). Exosome size and concentration were verified using nanoparticle tracking analysis NTA, NanoSight NS300, Malvern Panalytical, UK) and transmission electron microscopy TEM,

Zeiss EM10C, Germany). The presence of miRNA-143 in exosomes was confirmed by reverse transcription polymerase chain reaction RT-PCR). RNA was extracted from exosomes using TRIzol Invitrogen, Thermo Fisher Scientific), and RT-PCR was performed using miRNA-143-specific primers.

Exosome Transfer

Purified exosomes were quantified by protein content using a BCA assay Pierce, Thermo Fisher Scientific) and added to untreated HT-29 cells at a concentration of (100 µg/mL, adjust based on thesis data) in RPMI-1640 with exosome-depleted FBS Gibco) for 24 hours. Exosome-depleted FBS was prepared by ultracentrifugation at 100,000×g for 18 hours to remove endogenous exosomes.

Cell Viability Assay

Cell viability was assessed using the 3-(4,5-dimethylthiazol-2-yl)-2,5-diphenyltetrazolium bromide (MTT) assay. HT-29 cells were seeded at 5×10^3 cells/well in 96-well plates and treated with 5-FU, exosomes, or both. After treatment, cells were incubated with MTT solution (Sigma-Aldrich, 0.5 mg/mL) for 4 hours at 37°C. Formazan crystals were dissolved in DMSO, and absorbance was measured at 570 nm using a microplate reader (Bio-Rad, Hercules, CA, USA). Viability was calculated as a percentage relative to untreated controls.

Gene Expression Analysis

Total RNA was extracted from treated and control HT-29 cells using TRIzol reagent (Invitrogen). RNA quality was assessed by NanoDrop 2000 (Thermo Fisher Scientific), and 1 µg of RNA was reverse-transcribed into cDNA using the RevertAid First Strand cDNA Synthesis Kit (Thermo Fisher Scientific). Real-time quantitative PCR (qPCR) was performed on an ABI 7500 system (Applied Biosystems, Foster City, CA, USA) using SYBR Green PCR Master Mix (Takara Bio, Japan). Genes primer listed in table 1.

Table 1 . Genes primer

Genes		Sequence
MMP-7	forward	5'-GAGTGAGCTACAGTGGGAACA-3'
	reverse	5'-CTATGACGCGGAGTTAACAT-3'
BAX	forward	5'-CCCGAGAGGTCTTTTCCGAG-3'
	reverse	5'-CCAGCCCATGATGGTTCTGAT-3'
BCL2	forward	5'-GGTGGGGTCATGTGTGTGG-3'
	reverse	5'-CGGTTCAAGTACTCAGTCATCC-3'
GAPDH	forward	5'-GGAGCGAGATCCCTCCAAAAT-3'
	reverse	5'-GGCTGTTGTCATACTTCTCATGG-3'

Cycling conditions were: 95°C for 5 min, followed by 40 cycles of 95°C for 15 s, 60°C for 30 s, and 72°C for 30 s. Relative gene expression was calculated using the $\Delta\Delta C_t$ method, normalized to GAPDH.

Apoptosis Assays

Caspase-3/7 activity was measured using the Caspase-Glo 3/7 Assay Kit (Promega, Madison, WI, USA). Cells were seeded in 96-well white plates, treated, and incubated with Caspase-Glo reagent for 1 hour. Luminescence was measured using a Tecan Infinite M200 luminometer (Tecan, Männedorf, Switzerland). Apoptosis was further quantified by flow cytometry using the Annexin V-FITC/PI Apoptosis Detection Kit (BioLegend, San Diego, CA, USA). Treated cells were stained with Annexin V-FITC and propidium iodide (PI) per the manufacturer's protocol and analyzed on a BD FACSCalibur flow cytometer (BD Biosciences, San Jose, CA, USA). Data were processed using FlowJo software v10 (BD Biosciences).

ROS Measurement

Intracellular reactive oxygen species (ROS) levels were measured using the 2',7'-dichlorofluorescein diacetate (DCFH-DA) assay (Sigma-Aldrich). Cells were seeded in 96-well black plates, treated, and incubated with 10 µM DCFH-DA for 30 minutes at 37°C. Fluorescence was measured at 485 nm excitation/535 nm emission using a Tecan Infinite F200 fluorometer. ROS levels were expressed as fold change relative to controls.

confirmed in both images. These findings indicate the successful isolation of exosomes.

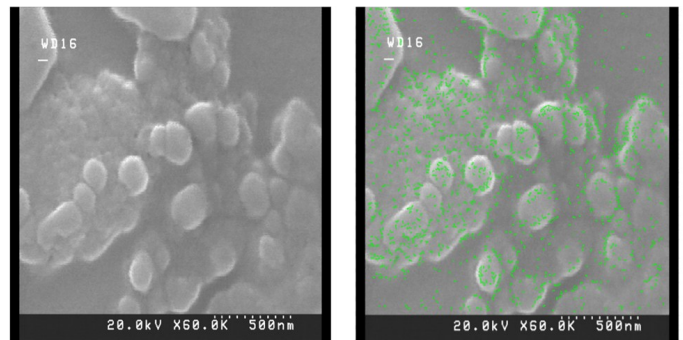


Figure 4. Scanning Electron Microscopy (SEM) Image of Exosomes Isolated from HT-29 Cells. Spherical particles with sizes ranging from 30 to 150 nm are observed on the surface, consistent with the known characteristics of exosomes. This image confirms the presence and relative purity of the isolated exosomes.

Confirmation of miRNA-143 Presence in Exosomes from 5-FU-Treated Cells Using PCR

The results of the PCR reaction demonstrated that miRNA-143 is significantly expressed in exosomes isolated from 5-FU-treated cells. The corresponding PCR product was observed at approximately 70 base pairs, consistent with the predicted size for miRNA-143 (Fig 5).

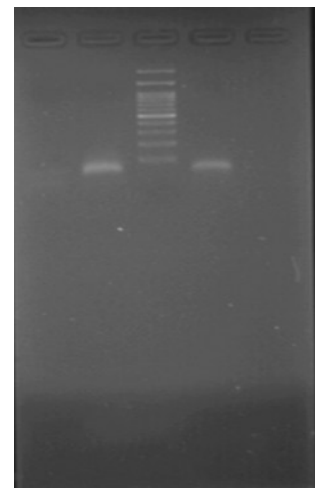


Figure 5. PCR Products with miRNA-143 Primer

Evaluation of miRNA-143 Expression in Isolated Exosomes

In this study, the expression level of miRNA-143 in exosomes extracted from biological samples was investigated. Exosomes, as extracellular vesicles, play a significant role in the transfer of genetic information, including miRNAs. miRNA-143 is a regulatory microRNA involved in metabolic

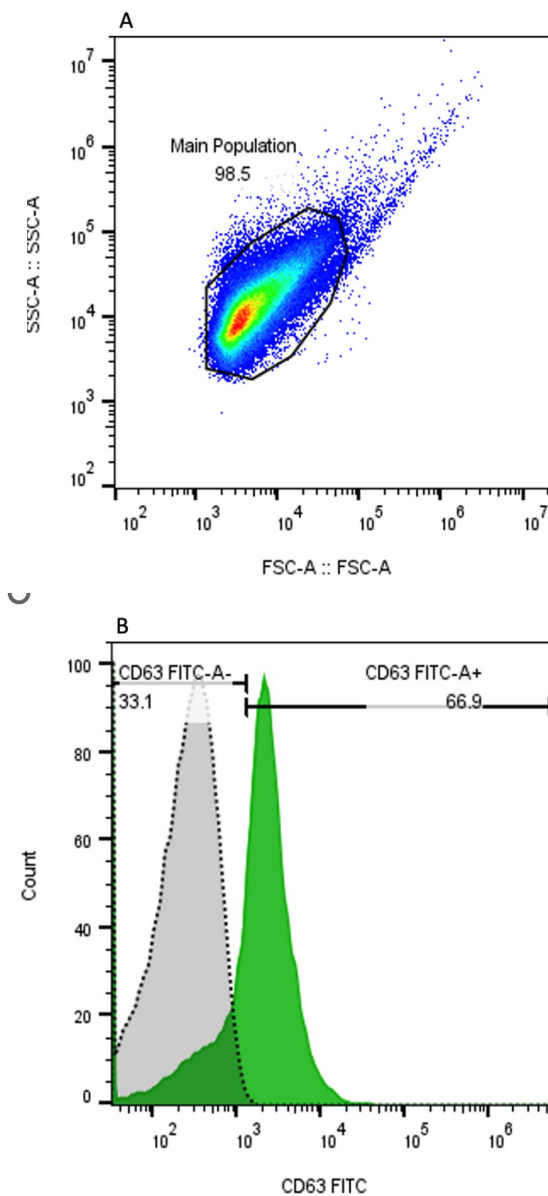


Figure 3. Flow Cytometry Histogram and Scatter Plot of Flow Cytometry Data for the 5-FU-CD63.fcs Sample. a) Fluorescence intensity of FITC corresponding to the anti-CD63 antibody (CD63-FITC-A), indicating the level of CD63 expression. b) A density plot in the style of a heatmap, illustrating the density of events (particles).

Verification of Exosomes Isolated from 5-FU-Treated HT-29 Cells Using Scanning Electron Microscopy (SEM)

Figure 4 (right image) displays multiple vesicular structures highlighted in green. These structures exhibit a spherical or oval shape, fall within the approximate size range of exosomes (30 to 150 nm), and their morphological characteristics are consistent with exosomes isolated from HT-29 cells. Based on the analyzed SEM images, the presence of spherical particles with appropriate sizes can be

Statistical Analysis

Experiments were performed in triplicate, and data are presented as mean \pm standard deviation (SD). Statistical analysis was conducted using SPSS v.25 (IBM, Armonk, NY, USA). Differences between groups were assessed by one-way analysis of variance (ANOVA) with Tukey's post-hoc test or Student's t-test for pairwise comparisons. A p-value <0.05 was considered statistically significant.

Ethics

This study was approved by the Institutional Review Board of Islamic Azad University, Science and Research Branch, Tehran, Iran (IRB No. (IR.IAU.SRB.REC.1402.001)).

Results

Culturing of HT-29 Cancer

Cells HT-29 cancer cells were obtained from the National Center for Genetic and Biological Resources and used for this study. Figure 1 illustrates the morphology and density of these cells.

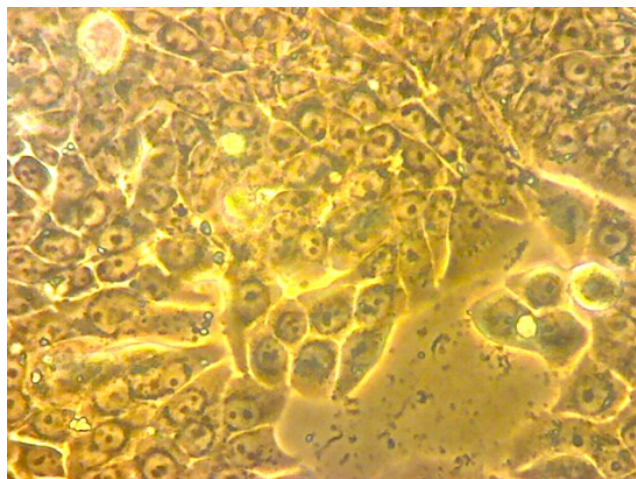


Figure 1. Morphology and Density of HT-29 Cancer Cells

Treatment of HT-29 Cancer Cells with 5-FU

The cells were incubated with increasing concentrations (0 to 20 μ M) of 5-FU for 24 and 48 hours. Cell viability was assessed using the MTT assay. The results indicate that all 5-FU concentrations above 1 mM significantly reduced cell viability

(Fig 2). The IC₅₀ values for 5-FU were determined to be 11.84 μ M and 3.727 μ M for 24 and 48 hours, respectively.

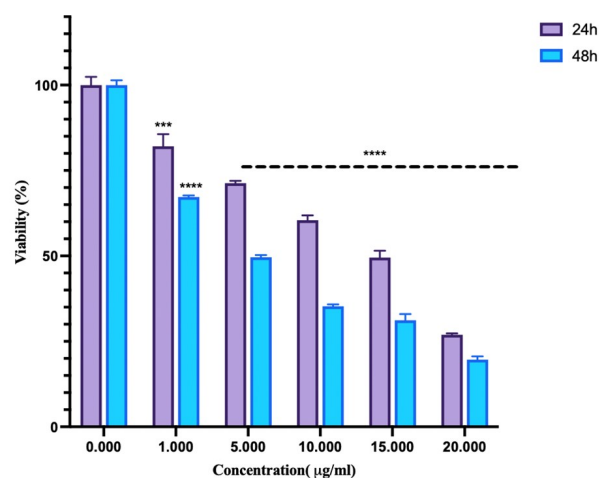


Figure 2. Viability of HT-29 Colorectal Cancer Cells Treated with 5-FU Each data point represents the mean \pm SEM relative to untreated control cells. ** Statistically significant compared to control at $p < 0.01$. *** Statistically significant compared to control at $p < 0.001$. **** Statistically significant compared to control at $p < 0.0001$

Verification of Exosomes Isolated from 5-FU-Treated HT-29 Cells Using the CD63 Marker

Based on Figure 3A, the presence of 98.5% of particles in the main population indicates high purity and desirable uniformity of the isolated particles. These particles may include exosomes or other extracellular vesicles. This finding confirms the accuracy of the isolation process and the satisfactory quality of the sample in terms of size, granularity, and particle homogeneity.

Additionally, the results of Figure 3B clearly demonstrate that approximately 66.9% of the particles in the sample exhibit positive CD63 expression, a marker widely recognized as specific for exosomes. This level of expression confirms the successful isolation of exosomes from 5-FU-treated HT-29 cells and the acceptable purity of the extracted exosomal population.

pathways, cell differentiation, and tumor suppression. Exosomes were isolated using standard precipitation methods or commercial kits, and their quality was verified. Total RNA was extracted, and miRNA-143 expression was assessed using quantitative real-time PCR (qRT-PCR). The results showed that miRNA-143 expression in exosomes was significantly higher when combined with 5-FU treatment, leading to an increase in microRNA expression (Fig 6).

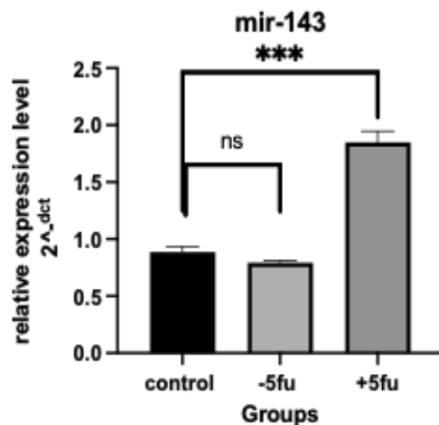


Figure 6. Evaluation of miRNA-143 Expression

Treatment of HT-29 Cells with miRNA-143-Loaded Exosomes

To evaluate the antiproliferative effect of miRNA-143-loaded exosomes on HT-29 cell line, cell viability was assessed following treatment with various concentrations 1, 5, 10, 15, and 20 $\mu\text{g/ml}$ for 24 and 48 hours. The results indicated a dose- and time-dependent reduction in cell viability. According to the data presented in Figure 4-2, the half-maximal inhibitory concentration (IC_{50}) values for 24 and 48 hours were calculated as 2.460 and 0.8684 $\mu\text{g/ml}$, respectively, demonstrating the high efficacy of these exosomes in suppressing the growth of HT-29 cancer cells (Fig7).

Morphological Changes in HT-29 Cells Following Treatment with miRNA-143-Loaded Exosomes

After treatment of HT-29 colorectal cancer cells

with miRNA-143-loaded exosomes ($\text{IC}_{50}/48$), distinct morphological alterations were observed.

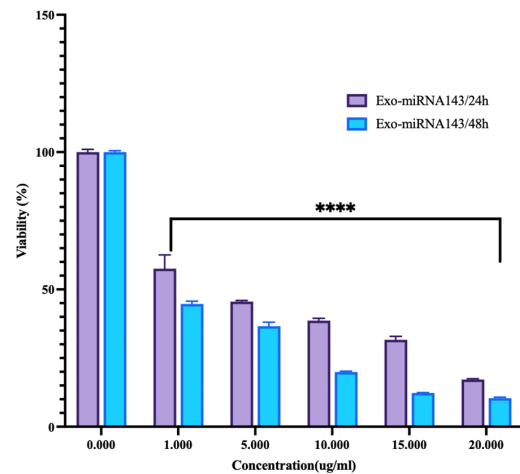


Figure 7. Viability of HT-29 Colorectal Cancer Cells Treated with miRNA-143-Loaded Exosomes Each data point represents the mean \pm SEM relative to untreated control cells. ** Statistically significant compared to control at $p < 0.01$ *** Statistically significant compared to control at $p < 0.001$ **** Statistically significant compared to control at $p < 0.0001$

Control cells (untreated) exhibited a regular epithelial shape, uniform monolayer growth, and strong adherence to the culture surface. In contrast, treated cells showed a marked reduction in adhesion, decreased cell density, and a transition to rounded and compact shapes. In some cases, cells detached from the substrate and appeared suspended in the medium, which may indicate the initiation of apoptosis (Fig 8).

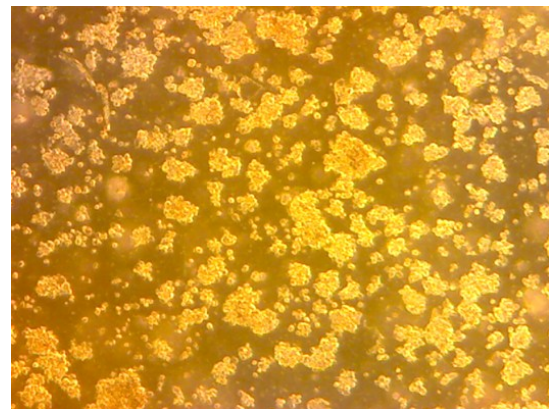


Figure 8. Phase-Contrast Microscopy Images of HT-29 Cells Before Treatment with miRNA-143-Loaded Exosomes In treated cells, notable changes were observed including reduced adhesion, cell rounding, decreased cell density, and the presence of suspended cells in the medium—indicative of apoptosis induction and the cytotoxic effects of the exosomes on cancer cells.

Analysis of Bax, Bcl-2, and MMP-7 Gene Expression Following Treatment of Colon Cancer Cells with miRNA-143-Loaded Exosomes

Gene expression analysis revealed that BAX expression significantly decreased after treatment with exosomes ($p = 0.0198$). MMP-7 expression also declined, although the reduction was not statistically significant. In contrast, BCL-2 expression showed a significant increase (Fig 9).

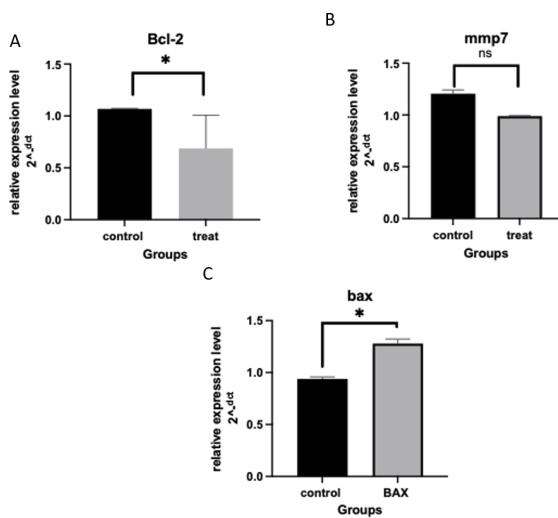


Figure 9. Analysis of BAX, MMP-7, and BCL-2 Gene Expression Following Treatment

Assessment of Caspase-3/7 Activity Following Treatment of Colon Cancer Cells with miRNA-143-Loaded Exosomes

The results of caspase-3/7 activity assay (Figure 9) demonstrated a significant increase in enzymatic activity following treatment of colon cancer cells with miRNA-143-loaded exosomes. Specifically, caspase-3/7 activity in treated cells was more than 1.5-fold higher compared to the untreated control group. Caspases 3 and 7 are key enzymes in the apoptotic pathway (programmed cell death), and their activation indicates the initiation or progression of apoptosis within cells. The marked elevation in caspase activity in response to exosome treatment suggests that these exosomes can effec-

tively induce caspase-dependent cell death pathways, thereby reducing the survival of cancer cells (Fig 10).

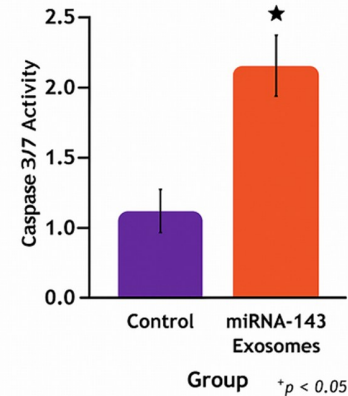


Figure 10. Caspase 3/7 activity following treatment of H-29 Colorectal cancer cells with MiRna-143 exosomes

Assessment of ROS Activity Following Treatment of Colon Cancer Cells with miRNA-143-Loaded Exosomes

Flow cytometry analysis revealed a significant reduction in the percentage of viable PI-) cells following treatment with isolated exosomes. Specifically, only 9.69% of the cells remained viable in the treated group, compared to 15.5% in the untreated control group. This reduction suggests a cytotoxic effect exerted by the exosomes (Fig 11). Furthermore, evaluation of reactive oxygen species (ROS) levels using the DCFH-DA probe demonstrated a marked increase in mean fluorescence intensity (MFI) in the exosome-treated group, reaching 9629, in contrast to 3301 in the control group. These findings indicate that exosomes can effectively induce oxidative stress in cancer cells and may play a critical role in regulating ROS-mediated cell death pathways (Fig 12).

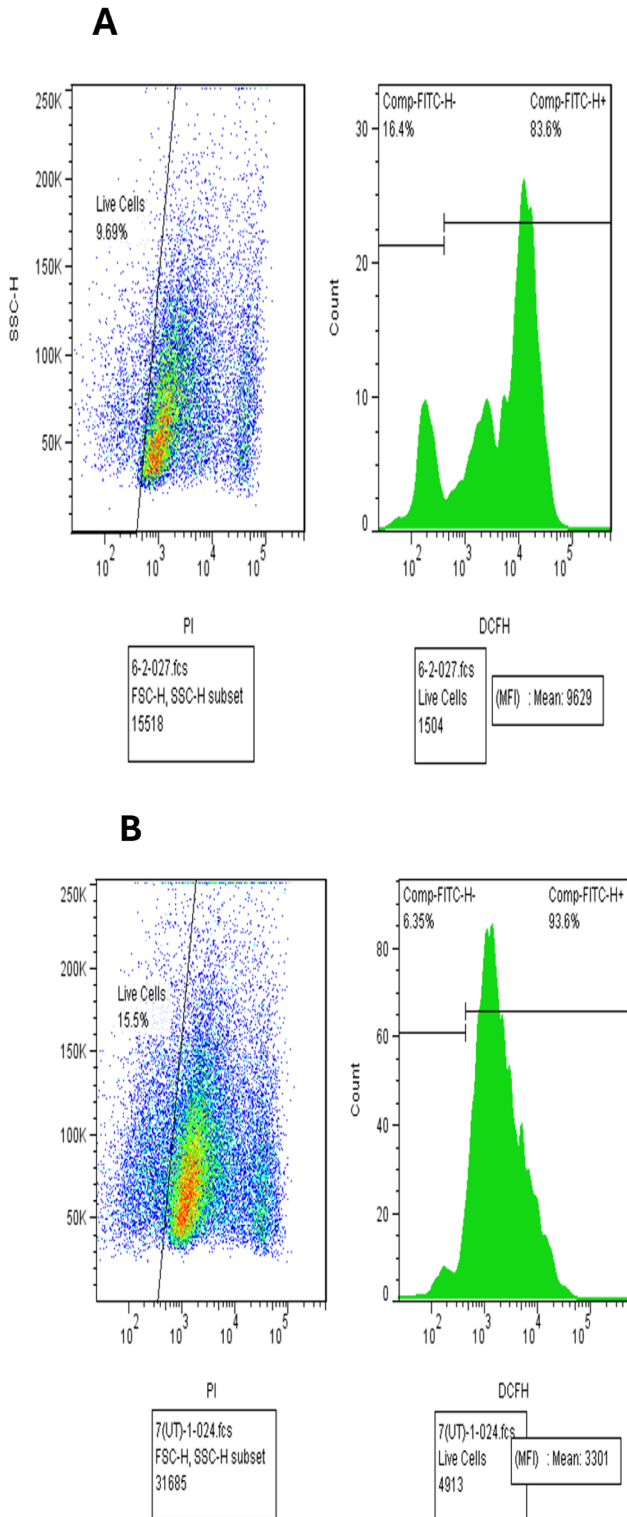


Figure 11. Flow cytometry analysis of cell viability and reactive oxygen species (ROS) production in exosome-treated cells (A) and the untreated control group (B).

Discussion

Colorectal cancer (CRC) ranks as the second most common cause of cancer-related death globally, arising from malignant transformations in the colon or rectum (43). Among CRC cases, approxi-

mately 72% originate in the colon and 28% in the rectum (44).

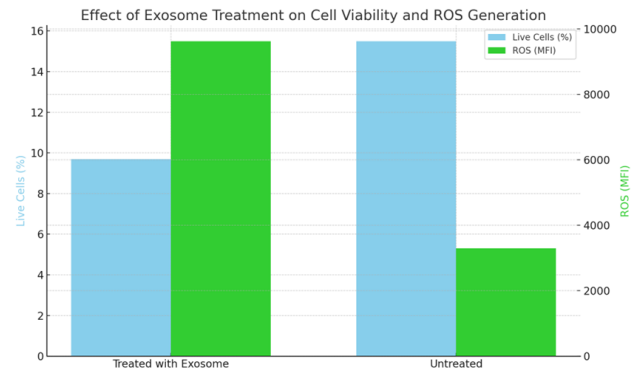


Figure 12. Flow Cytometry Analysis of Cell Viability and Reactive Oxygen Species (ROS) Production in Exosome-Treated Cells and Untreated Control Group

The vast majority—over 90%—are adenocarcinomas that develop from glandular epithelial cells lining these regions. The disease initiates when these cells undergo genetic or epigenetic alterations that drive uncontrolled growth and survival. This abnormal proliferation leads to the formation of benign polyps, which can evolve into invasive adenocarcinomas and eventually metastasize to distant organs over time. Common clinical manifestations include rectal bleeding, altered bowel habits, abdominal discomfort and bloating, fatigue, anemia, and unexplained weight loss (44).

5-Fluorouracil (5-FU) remains a cornerstone chemotherapeutic agent known to enhance survival across various malignancies, with its most pronounced efficacy observed in CRC (45). Its active metabolites interfere with DNA and RNA synthesis by targeting the folate metabolic pathway (46). Despite its widespread use, the response rate to 5-FU in advanced CRC is relatively low, ranging from 10–15%. Although combining 5-FU with agents like irinotecan and oxaliplatin has shown improved outcomes, it also leads to increased toxicity (46).

Exosomes—small, membrane-bound vesicles measuring 40 to 140 nm—are secreted by cells and function as molecular messengers.

Their structural similarity to the parent cell membrane facilitates targeted delivery to specific tissues. Surface proteins such as major histocompatibility complexes help the immune system differentiate between endogenous and foreign particles. Exosomes can be isolated from various biological fluids, including plasma, urine, breast milk, and blood (47).

MicroRNAs (miRNAs) are short, non-coding RNA molecules that regulate gene expression by binding to target mRNAs, leading to translational repression or degradation (189). A single miRNA can influence hundreds of mRNA targets, thereby modulating numerous genes involved in interconnected biological pathways (48).

Among these, miR-143 and miR-145—located on chromosome 5q32–33—have been shown to be downregulated in several cancers, including CRC (190–192). Michael et al. were the first to report this association in 2003, highlighting reduced levels of miR-143/145 in colorectal tumor tissues compared to normal samples (49). These miRNAs are widely recognized as tumor suppressors. In CRC, diminished expression of miR-143 correlates with elevated levels of DNMT3A, a DNA methyltransferase that contributes to tumor progression through epigenetic modifications (5). Additionally, Hu et al. demonstrated that the long non-coding RNA PART1 competes with DNMT3A for miR-143 binding, suggesting PART1 may represent a viable therapeutic target (50).

The present study was designed to explore the regulatory role of miRNA-143-enriched exosomes in HT-29 colorectal cancer cells, particularly under 5-FU treatment. The investigation focused on how these exosomes influence the expression of genes involved in apoptosis (BAX, BCL2) and metastasis (MMP-7), aiming to determine whether miRNA-143 could enhance chemotherapy efficacy or miti-

gate drug resistance.

To achieve this, exosomes containing miRNA-143 were extracted from the culture medium of 5-FU-treated cells. PCR analysis confirmed the presence of miRNA-143 within these vesicles. The exosomes were then introduced to HT-29 cells, and cell viability was assessed using the MTT assay. Total RNA was isolated to quantify the expression of MMP-7, BAX, and BCL2 via Real-Time PCR. Additional assays measured caspase-3/7 activity, flow cytometry was used to evaluate apoptosis, and intracellular ROS levels were analyzed.

Findings revealed that miRNA-143-enriched exosomes significantly reduced HT-29 cell viability. The MTT assay indicated a marked decline in metabolic activity. MMP-7 expression, associated with invasion and metastasis, was suppressed, while pro-apoptotic BAX was upregulated and anti-apoptotic BCL2 was downregulated. Caspase activity and flow cytometry further confirmed increased apoptotic activity in treated cells.

These results align with recent research exploring exosome-based cancer therapies. For instance, Bethany N. Hannafon investigated the impact of docosahexaenoic acid (DHA) on breast cancer cells via exosomal modulation. DHA treatment enhanced exosome release and altered miRNA profiles in MCF7 and MDA-MB-231 cells, notably increasing tumor-suppressive and anti-angiogenic miRNAs such as let-7a, miR-23b, miR-27a/b, miR-21, let-7, and miR-320b—changes not observed in normal MCF10A cells. These miRNAs were transferred to endothelial cells, where they inhibited angiogenesis-related genes (e.g., PLAU, AMOTL1, NRP1, ETS2) and suppressed tube formation. Silencing Rab27A reversed these effects, underscoring DHA's anti-angiogenic potential through exosomal miRNA transfer (51).

Another study explored the biogenesis, transport,

and diagnostic utility of exosomal miRNAs in CRC. Evidence increasingly supports the role of specific miRNAs—such as miR-21, miR-150, miR-192, let-7a, miR-223, and miR-23a—as non-invasive biomarkers for early detection and prognosis in CRC patients (52).

In research by Kyeongsoo Jeon et al., exosomes derived from human cells were used to deliver miRNA-497 to non-small cell lung cancer (NSCLC) models. Both 2D and 3D microfluidic systems mimicking in vivo conditions demonstrated that miR-497-enriched exosomes suppressed A549 cell proliferation and downregulated angiogenesis-related genes including YAP1, HDGF, CCNE1, and VEGF-A. In endothelial cells (HUVECs), VEGF-A-induced sprouting was significantly inhibited. Co-culture experiments revealed reduced tube formation and cancer cell migration, suggesting that miR-497-loaded exosomes can concurrently inhibit tumor growth and angiogenesis. This approach, when combined with microfluidic platforms, offers a promising strategy for targeted cancer therapy (53).

In a separate study, Mansour Al-Moha and colleagues examined the effects of exosomes derived from mesenchymal stem cells (MSCs) exposed to oxidative stress (via H₂O₂ treatment) in breast cancer models. While prior studies yielded conflicting results regarding MSCs' influence on tumor progression, this investigation showed that exosomes from stressed MSCs (St-MSC Exo) elevated VEGF expression and EMT markers, promoting tumor growth through STAT3 signaling. Conversely, exosomes from untreated MSCs suppressed STAT3 phosphorylation and VEGF expression. Treated cancer cells also exhibited increased NF- κ B activation and ROS production. In vitro, St-MSC Exo enhanced endothelial cell proliferation, migration, and angiogenesis, while in vivo experi-

ments confirmed their tumor-promoting effects (54).

Conclusion

Exosomes loaded with miRNA-143 significantly enhance the anti-cancer effects of 5-FU in HT-29 CRC cells. They help lower cell viability, downregulate MMP-7, upregulate BAX, reduce BCL2, and increase ROS levels. Overall, these findings indicate that exosomal miRNA-143 could be a novel adjunct therapy to overcome chemoresistance in CRC, meriting further exploration.

Acknowledgments

With sincere gratitude to the colleagues at Kimia Andisheh Teb Medical and Molecular Laboratory Research Co. for their invaluable guidance throughout the cellular and molecular experiments.

Funding

Supportd by authors

Conflicts of Interest

The authors declare no conflicts of interest.

References

11. Siegel RL, et al. Cancer statistics, 2022. *CA Cancer J Clin.* 2022;721):7-33.
2. Varol U, et al. Markers to predict the efficacy of bevacizumab in the treatment of metastatic colorectal cancer. *Tumori Journal.* 2014;1004):370-376.
3. Longley DB, Harkin DP, Johnston PG. 5-fluorouracil: mechanisms of action and clinical strategies. *Nat Rev Cancer.* 2003;35):330-338.
4. Zhang N, et al. 5-Fluorouracil: mechanisms of resistance and reversal strategies. *Molecules.* 2008;138):1551-1569.
5. Radenković N, et al. Resistance to 5-fluorouracil: The molecular mechanisms of development in colon cancer cells. *Eur J Pharmacol.* 2024;983:176979.
6. Shah MY, Calin GA. The mix of two worlds: non-coding RNAs and hormones. *Nucleic Acid Ther.* 2013;231):2-8.
7. Hur K. MicroRNAs: promising biomarkers for diagnosis and therapeutic targets in human colorectal cancer metastasis. *BMB Rep.* 2015;484):217.
8. Chen J, Wang MB. The roles of miRNA-143 in colon cancer and therapeutic implications. *Transl Gastrointest*

10. Zhang Y, et al. Profiling of 95 microRNAs in pancreatic cancer cell lines and surgical specimens by real-time PCR analysis. *World J Surg.* 2009;33(4):698.
11. Ng EK, et al. MicroRNA-143 is downregulated in breast cancer and regulates DNA methyltransferases 3A in breast cancer cells. *Tumour Biol.* 2014;35(3):2591-2598.
12. Qian X, et al. MicroRNA-143 inhibits tumor growth and angiogenesis and sensitizes chemosensitivity to oxaliplatin in colorectal cancers. *Cell Cycle.* 2013;12(9):1385-1394.
13. Qian X, et al. MicroRNA-143 inhibits tumor growth and angiogenesis and sensitizes chemosensitivity to oxaliplatin in colorectal cancers. *Cell Cycle.* 2013;12(9):1385-1394.
14. Hernández R, Sánchez-Jiménez E, Melguizo C, Prados J, Rama AR. Downregulated microRNAs in the colorectal cancer: diagnostic and therapeutic perspectives. *BMB Rep.* 2018;51(11):563–571. doi:10.5483/BMBRep.2018.51.11.116
15. Shirzad S, Eterafi M, Karimi Z, Barazesh M. MicroRNAs involved in colorectal cancer: a rapid mini-systematic review. *BMC Cancer.* 2025;25:934. doi:10.1186/s12885-025-14343-1
16. Valenzuela G, Contreras HR, Marcelain K, Burotto M, González-Montero J. Understanding microRNA-mediated chemoresistance in colorectal cancer treatment. *Int J Mol Sci.* 2025;26(3):1168. doi:10.3390/ijms26031168
17. Xiong B, Huang Q, Zheng H, Lin S, Xu J. Recent advances in microRNAs and metabolic reprogramming in colorectal cancer. *Front Oncol.* 2023;13:1165862. doi:10.3389/fonc.2023.1165862
18. Review The role of miRNAs in colorectal cancer progression and chemoresistance. *Biomed Pharmacother.* 2021.
19. Kalluri R, LeBleu VS. The biology, function, and biomedical applications of exosomes. *Science.* 2020;367(6478):eaau6977.
20. Grange C, et al. Microvesicles released from human renal cancer stem cells stimulate angiogenesis and formation of lung premetastatic niche. *Cancer Res.* 2011;71(15):5346-5356.
21. Ratajczak J, et al. Embryonic stem cell-derived microvesicles reprogram hematopoietic progenitors: evidence for horizontal transfer of mRNA and protein delivery. *Leukemia.* 2006;20(5):847-856.
22. Hannafon BN, Ding WQ. Intercellular communication by exosome-derived microRNAs in cancer. *Int J Mol Sci.* 2013;14(7):14240-14269.
23. Zhang H, et al. MicroRNA-143 targets MACC1 to inhibit cell invasion and migration in colorectal cancer. *Mol Cancer.* 2012;11:23.
24. Konda B, Shum H, Rajdev L. Anti-angiogenic agents in metastatic colorectal cancer. *World J Gastrointest Oncol.* 2015;7(7):71.
25. Borralho PM, Kren BT, Castro RE, da Silva IB, Steer CJ, Rodrigues CMP. MicroRNA-143 reduces viability and increases sensitivity to 5-fluorouracil in HCT116 human colorectal cancer cells. *FEBS J.* 2009;276(22):6689–6700. doi:10.1111/j.1742-4658.2009.07383.x
26. Chen J, Wang MB. The roles of miRNA-143 in colon cancer and therapeutic implications. *Transl Gastrointest Cancer.* 2012;12(1):169-174.
27. Hur K. MicroRNAs: promising biomarkers for diagnosis and therapeutic targets in human colorectal cancer metastasis. *BMB Rep.* 2015;48(4):217.
28. Ii M, et al. Role of matrix metalloproteinase-7 (matrilysin) in human cancer invasion, apoptosis, growth, and angiogenesis. *Exp Biol Med.* 2006;231(1):20-27.
29. Noë V, et al. Release of an invasion promoter E-cadherin fragment by matrilysin and stromelysin-1. *J Cell Sci.* 2001;114(1):111-118.
30. Chu D, et al. Matrix metalloproteinase-7 expression is associated with poor prognosis in colorectal cancer patients. *Int J Clin Exp Pathol.* 2013;6(11):2253-2260.
31. Siegel RL, et al. Cancer statistics, 2022. *CA Cancer J Clin.* 2022;72(1):7-33.
32. Jürgensmeier JM, et al. Bax directly induces release of cytochrome c from isolated mitochondria. *Proc Natl Acad Sci.* 1998;95(9):4997-5002.
33. Wei MC, et al. Proapoptotic BAX and BAK: a requisite gateway to mitochondrial dysfunction and death. *Science.* 2001;292(5517):727-730.
34. Youle RJ, Strasser A. The BCL-2 protein family: opposing activities that mediate cell death. *Nat Rev Mol Cell Biol.* 2008;9(1):47-59.
35. Raisova M, et al. The Bax/Bcl-2 ratio determines the susceptibility of human melanoma cells to CD95/Fas-mediated apoptosis. *J Invest Dermatol.* 2001;117(2):333-340.
36. The BCL2 family: from apoptosis mechanisms to new advances in cancer therapy. *Signal Transduct Target Ther.* 2025.
37. Synergistic Inhibition of Colon Cancer Cell Proliferation via aerobic glycolysis. *ACS Omega.* 2025.
38. Exploring Butein's anticancer potential in colorectal cancer. *J Ethnopharmacol.* 2024.
39. Metformin induces apoptosis in TRAIL-resistant colorectal cancer cells. *Biochim Biophys Acta Mol Basis Dis.* 2024.
40. ABCE1 facilitates tumour progression via aerobic glycolysis and apoptosis evasion in colorectal cancer. *Sci Rep.* 2025.
41. Guo H, et al. MicroRNA-143 promotes apoptosis of osteosarcoma cells by caspase-3 activation via targeting Bcl-2. *Oncol Lett.* 2016;12(1):521-526.
42. Zheng P, et al. Tumor-associated macrophage-derived exosomes promote the migration of gastric cancer cells by transfer of functional Apolipoprotein E. *Cell Death Dis.* 2018;9(4):434.
43. Xi, Y. and P. Xu, Global colorectal cancer burden in 2020 and projections to 2040. *Translational oncology,* 2021. 14(10): p. 101174.
44. Alzahrani, S.M., H.A. Al Doghaither, and A.B. Al-Ghafari, General insight into cancer: An overview of colorectal cancer. *Molecular and clinical oncology,* 2021. 15(6): p. 271.
45. Longley, D.B., D.P. Harkin, and P.G. Johnston, 5-fluorouracil: mechanisms of action and clinical strategies. *Nature reviews cancer,* 2003. 3(5): p. 330-338.
46. Afzal, S., et al., MTHFR polymorphisms and 5-FU-based adjuvant chemotherapy in colorectal cancer. *Annals of oncology,* 2009. 20(10): p. 1660-1666.
47. Nicolini, A., P. Ferrari, and P.M. Biava, Exosomes and cell communication: from tumour-derived exosomes and their role in tumour progression to the use of exosomal cargo for cancer treatment. *Cancers,* 2021. 13(4): p. 822.

-
48. Valeri, N., C.M. Croce, and M. Fabbri, Pathogenetic and clinical relevance of microRNAs in colorectal cancer. *Cancer genomics & proteomics*, 2009. 6(4): p. 195-204.
 49. Michael, M.Z., et al., Reduced accumulation of specific microRNAs in colorectal neoplasia. *Molecular cancer research*, 2003. 1(12): p. 882-891.
 50. u, Y., et al., PART-1 functions as a competitive endogenous RNA for promoting tumor progression by sponging miR-143 in colorectal cancer. *Biochemical and Biophysical Research Communications*, 2017. 490(2): p. 317-323.
 51. Hannafon, B.N., et al., Exosome-mediated microRNA signaling from breast cancer cells is altered by the anti-angiogenesis agent docosahexaenoic acid (DHA). *Molecular cancer*, 2015. 14(1): p. 133
 52. Hosseini, M., et al., Exosome-encapsulated microRNAs as potential circulating biomarkers in colon cancer. *Current pharmaceutical design*, 2017. 23(11): p. 1705-1709.
 53. Jeong, K., et al., Exosome-mediated microRNA-497 delivery for anti-cancer therapy in a microfluidic 3D lung cancer model. *Lab on a Chip*, 2020. 20(3): p. 548-557.
 54. Almouh, M., et al., Exosomes released by oxidative stress-induced mesenchymal stem cells promote murine mammary tumor progression through activating the STAT3 signaling pathway. *Molecular and Cellular Biochemistry*, 2024. 479(12): p. 3375-3391.